

Study of a Gradual Rectangular Bragg Grating on Graphene Nano-Ribbon Assisted Mid-Infrared Band Stop, Band-pass Filter

Alireza Tavousi¹ Mina Ranjbar-Torkamani²

1. Department of Electrical Engineering, Velayat University, Iranshahr, Iran (a.tavousi@velayat.ac.ir)
2. Department of Electrical Engineering, Velayat University, Iranshahr, Iran

Abstract-Band-Pass and band-stop filters are basic filters in communications and electronics industry. Here in this study we proposed a band-pass filter using gradual increasing-decreasing graphene nano-ribbon (GNR) assisted Bragg-gratings with enhanced benefit from special abilities in light confinement to control mid-infrared transmissions. Application of conventional semiconductor based Bragg-gratings for mid-infrared requires a μm -scale footprint, while novel on-chip integrated circuits only accept nm-scale devices. The solution to this need is to integrate the Bragg-grating with a GNR. The doping level and electron relaxation time are assumed as empirical values for this study to avoid the limitation factors on device performance. The findings of this report quantitatively demonstrate high performance of this plasmonic based GNR assisted device.

Keywords: Band-pass filter; Gradual Bargg-Grating; Graphene Nano Ribbon.

1 Introduction

All-optical filters are in the middle class of most wanted electronic devices for multiple range of frequency applications [1-5]. Among those class, mid-infrared devices have attracted huge devotion of researchers [6-9]. Integration the need of mid-infrared class tools and nm-scale requirement of current electronic devices, brings forward the graphene as a unique opportunity. Graphene is an important material for this domain because of it fascinating optical, electrical, and thermal characteristics [10, 11].

Graphene comes in a two dimensional honeycomb lattice of single layer carbon atoms which tunes either by electrostatic excitation of electron-hole pairs or chemical doping injection. Because of large dopant injection number, its Ohmic losses decrease and its conductivity properties change. In mid-infrared wavelengths, surface plasmon polariton (SPP) propagation becomes possible on the edges graphene nano ribbons (GNR) [12]. Its electrical conductivity can be modified by aforementioned methods which in turn results in refractive index deviations. In this manner, device tuning is not limited to design and fabrication process steps.

Using GNRs, numerous structures have already been designed such as optical switches [13, 14], filters [15-17], tuneable antennas [18], and so on. Here, an ultra-compact GNR based band-pass filter is proposed. It can be tuned in a way that its

transmission spectrum resonant peak can easily be tuned in real time.

In the following section, the theoretical rules, simulation codes and criteria, design respects and parameters are discussed. Section 3 presents the result and is followed by discussions about spectral behaviour of the mid-infrared proposed band pass filter with respect to chemical potential variations and/or geometrical dimension tuning. In the end, Section 4 concludes our study.

2 Design and Theory

The three-dimensional representation of the GNR-based band-pass filter is displayed in **Fig. 1**. It consists of a 20 nm wide graphene strip that goes throughout the device and acts as input/output. The multilayered gradual Si blocks are placed on top of this strip.

TABLE I. Simulation parameters of proposed structure.

Parameter	Symbol	Values	Unit
Period of grating blocks	L_1	30	nm
Period of air blocks	L_2	60	nm
Height of grating blocks	H	60	nm
Number of grating	N	4 to 14	-
Widths of the GNR	W_G	20	nm
Thickness of Si	T_{Si}	500	nm
Thickness of SiO ₂	T_{SiO_2}	50	nm
Chemical potential	μ_c	0.6	eV
Relaxation time	τ	0.3	eV
Temperature	T	300	°K

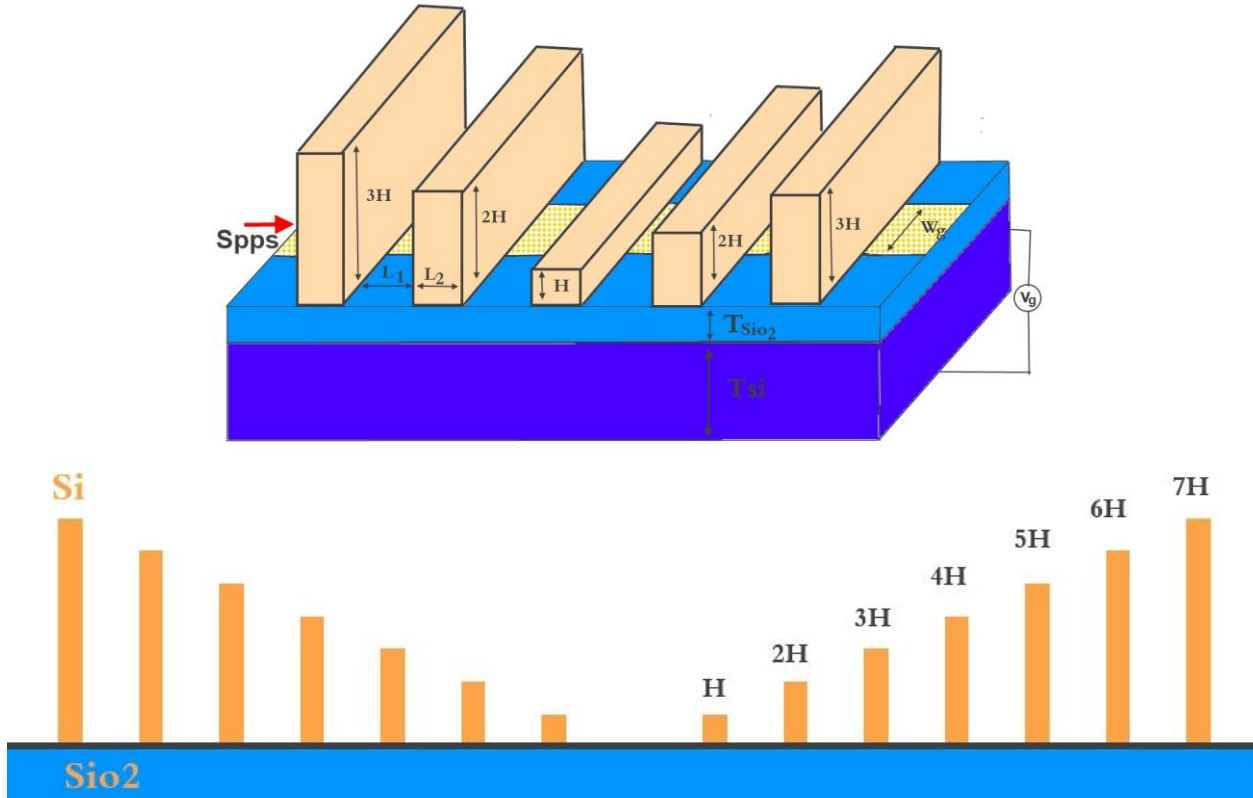


Figure 1. (a)The 3D representation of the GNR-based BPF, (b) Side view

The beneath of GNR, composed of highly-doped silicon slab stacked under a thin layer of silica. Geometrical values and physical parameters of proposed structure are summarized in **Table I**.

If a bias voltage applies between graphene and silicon slab, graphene's chemical potential varies, so if a broadband mid-infrared Gaussian wave excites the entrance port, quasi-SPPs are strongly animated along the edge of graphene layer. The relation between phase velocity (v_{ph}), optical excitation frequency (ω) and wave number (k) is governed by [19]:

$$v_{ph} = \frac{\omega}{k}. \quad (1)$$

Due to inverse relation of phase velocity and wave number which are functions of the medium, by increasing of the refractive index, the wavelength and phase velocity decrease. Graphene's chemical potential depends on the charge carrier absorption which are tuned by chemical dopant realization and/or electrostatic gating. Chemical potential of the graphene, μ_c , and

applied gating voltage, V_{bias} , are related as given [15]:

$$\mu_c = \sqrt{\frac{\pi \epsilon_0 \epsilon_r V_{bias}}{et}}, \quad (2)$$

where ϵ_0 and ϵ_r are permittivity of vacuum and relative permittivity SiO₂, e is the electron charge, and t is the thickness of Si substrate.

For numerical simulations of the current study, GNR spectral behaviour is displayed with random-phase approximation method [20, 21]. In this model, the optical response of graphene dynamics is described by Kubo formalism. It consists of two sections, the interband and intraband contributions, i.e. $\sigma_g = \sigma_{inter} + \sigma_{intra}$, where σ_g denotes the conductivity of graphene. The T is the temperature, \hbar is the reduced Plank's constant, and v_F is the Fermi velocity with value of 10^6 m/s [22, 23]. Generally, for zero wave vector (i.e. $k=0$ in the local limit) and by random-phase approximation (RPA), graphene's conductivity will simplify to [24]:

$$\sigma_g = \frac{2ie^2k_B T}{\pi h^2 [\omega + i\tau^{-1}]} \ln \left[2 \cosh \left[\frac{E_f}{2k_B T} \right] \right] + \frac{ie^2}{4\pi h} \ln \left[\frac{2E_f - h[\omega + i\tau^{-1}]}{2E_f + h[\omega + i\tau^{-1}]} \right] \quad (3)$$

The σ_g can be interpreted as a function of applied voltage V_{bias} . The σ_g and n_{eff} are related via [15]:

$$n_{\text{eff}} = \sqrt{\epsilon_r - \left(\frac{2\epsilon_r}{\sigma_g \eta_0} \right)^2} \quad (4)$$

where η_0 ($\sim 377\Omega$) is the impedance of the ambient around the graphene.

A vertical multilayered of Si/SiO₂/GNR along with a horizontal gradual Bragg grating is used to form the filter. Si and SiO₂ are supposed to have refractive indices of 3.45 and 1.44, respectively.

The simulations are performed using three-dimensional FDTD with a minimum mesh size of 0.01 nm to guarantee the validity of results as well

as preserving the time efficiency. The results are proficient under appropriate boundary conditions with embedded perfectly matched layers (PML).

3 Results and Discussions

Since immediate media around the GNR has direct effect on the acquired results, therefore 3D simulations are required. As an example, the thickness of the SiO₂ layer beneath the graphene layer has a significant impact on the shift of peak within transmission spectrum. By using denser thicknesses of substrate (at least 50 nm), this enslavement is correlated to invariant results. Furthermore, graphene Nano ribbons do support both wave guiding and edge modes [15]. If the width of the GNR goes to fewer than tens of nanometers, edge mode becomes the dominant mode. Moreover the edge modes have higher n_{eff} , which makes it suitable for filtering and transmission applications. Our studies within **figure 2** fully confirms the existence of these edge modes for our BPF.

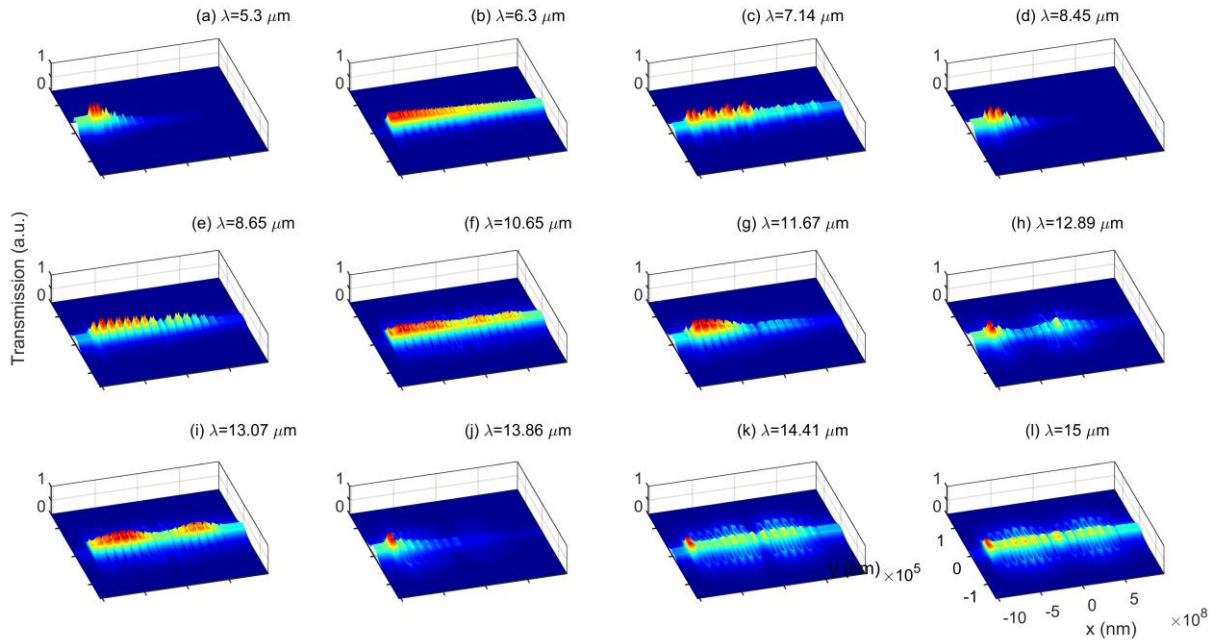


Figure 2: Representation of the E_z electric field of GNR's edge mode in a 14 blocks gradually arranged grating on top a GNR.

The Bragg-wavelength could be found from Bragg-scattering criteria as:

$$L_1 \text{Re}(n_{\text{eff}1}) + L_2 \text{Re}(n_{\text{eff}2}) = m\lambda_b/2 \quad (5)$$

where λ_b is the Bragg resonant wavelength, and m is an integer assumed to be 1. L_1 and L_2 are the high and low dielectric constants length, and creates the grating period together. The high dielectric material is silicon and the low dielectric material is air, respectively. The $\text{Re}(n_{\text{eff}1})$ and $\text{Re}(n_{\text{eff}2})$ are real part of mentioned high and low dielectric materials, respectively. According to this equation, the Bragg wavelength along with the transmission pass/stop window is easily tuned by changing these parameters.

Similarly to fiber Bragg grating, by accumulative growth of the number of periods (N_{Blocks}), it is expected that stop-band transition regions becomes more selective, where the centre of Bragg wavelength remains constant. This is verified for our structure, as shown in **Fig. 3**. Due to enhance n_{eff} of GNR, modulation effects are much stronger and thus only a few number of N_{Block} are required. For the sake of device smaller footprint, we have chosen the $N=4$ to 14 which results in a stop band around 9 to 11.5 μm .

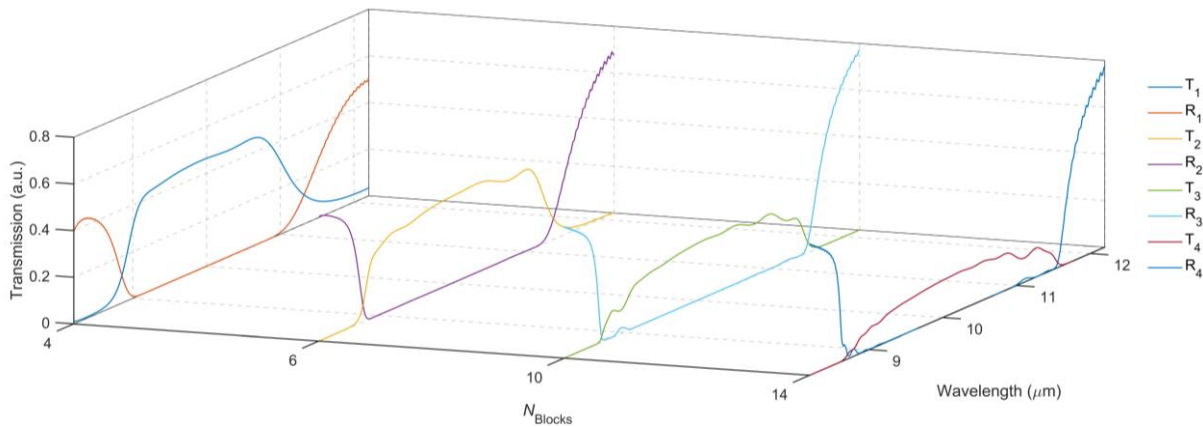


Figure 3: Transmission and reflection of the proposed BPF when configured according to Table I.

4 Conclusion

By means of gradual height increasing bragg grating, a GNR-assisted band stop-pass filter was designed. The transmission peak was easily tuned by altering the period of gradual height or scale Bragg grating. In addition, due to tune ability of GNR's effective index that occurs by introducing tiny variation in surface charge carrier density through applying a gate voltage, dynamic tuning was proposed for this filter.

References

- [1] A. Tavousi, M. A. Mansouri-Birjandi, M. Ghadrhan, and M. Ranjbar-Torkamani, "Application of photonic crystal ring resonator nonlinear response for full-optical tunable add-drop filtering," *Photonic Network Communications*, vol. 34, no. 1, pp. 131-139, 2017.
- [2] A. Tavousi and M. A. Mansouri-Birjandi, "Study on the similarity of photonic crystal ring resonator cavity modes and whispering-gallery-like modes in order to

design more efficient optical power dividers," *Photonic Network Communications*, vol. 32, no. 1, pp. 160-170, 2016.

- [3] M. A. Mansouri-Birjandi, A. Tavousi, and M. Ghadrhan, "Full-optical tunable add/drop filter based on nonlinear photonic crystal ring resonators," *Photonics and Nanostructures-Fundamentals and Applications*, vol. 21, pp. 44-51, 2016.
- [4] A. Tavousi and M. A. Mansouri-Birjandi, "Performance evaluation of photonic crystal ring resonators based optical channel add-drop filters with the aid of whispering gallery modes and their Q-factor," *Optical and Quantum Electronics*, vol. 47, no. 7, pp. 1613-1625, 2015.
- [5] A. Tavousi, M. A. Mansouri-Birjandi, and M. Saffari, "Add-Drop and Channel-Drop Optical Filters Based on Photonic Crystal Ring Resonators," *International Journal of Communications and Information Technology*, vol. 1, no. 2, pp. 19-24, 2012.
- [6] A. Tavousi, A. Rostami, G. Rostami, and M. Dolatyari, "Proposal for Simultaneous Two-Color Smith-Purcell Terahertz Radiation Through Effective Surface Plasmon Excitation," *IEEE Journal of Selected Topics in Quantum Electronics*, vol. 23, no. 4, pp. 1-9, 2017.



- [7] A. Tavousi, A. Rostami, G. Rostami, and M. Dolatyari, "3-D numerical analysis of Smith–Purcell-based terahertz wave radiation excited by effective surface plasmon," *Journal of Lightwave Technology*, vol. 33, no. 22, pp. 4640-4647, 2015.
- [8] A. Tavousi, A. Rostami, G. Rostami, and M. Dolatyari, "3-D Analysis of terahertz frequency multiplier excited due to interaction of convection electron beam and surface waves (Smith-Purcell Effect)," in *Photonics, Optics and Laser Technology (PHOTOPTICS), 2015 International Conference on*, 2015, vol. 2, pp. 34-39: IEEE.
- [9] A. Tavousi, A. Rostami, G. Rostami, and M. Dolatyari, "Smith-Purcell Based Terahertz Frequency Multiplier: Three Dimensional Analysis," in *Photoptics 2015*: Springer, 2016, pp. 145-155.
- [10] A. Farmani, M. Yavarian, A. Alighanbari, M. Miri, and M. H. Sheikhi, "Tunable graphene plasmonic Y-branch switch in the terahertz region using hexagonal boron nitride with electric and magnetic biasing," *Applied Optics*, vol. 56, no. 32, pp. 8931-8940, 2017.
- [11] A. Tavousi, M. A. Mansouri-Birjandi, and M. Janfaza, "Optoelectronic application of graphene nano-ribbon for mid-infrared band-pass filtering," *unpublished*, 2017.
- [12] M. Liu and X. Zhang, "Silicon photonics: Graphene benefits," *Nature Photonics*, vol. 7, no. 11, pp. 851-852, 2013.
- [13] A. Farmani, A. Zarifkar, M. H. Sheikhi, and M. Miri, "Design of a tunable graphene plasmonic-on-white graphene switch at infrared range," *Superlattices and Microstructures*, 2017.
- [14] M. Dragoman, D. Dragoman, F. Coccetti, R. Plana, and A. Muller, "Microwave switches based on graphene," *Journal of applied physics*, vol. 105, no. 5, p. 054309, 2009.
- [15] M. Janfaza, M. A. Mansouri-Birjandi, and A. Tavousi, "Tunable plasmonic band-pass filter based on Fabry–Perot graphene nanoribbons," *Applied Physics B*, vol. 123, no. 10, p. 262, 2017.
- [16] J. Tao, X. Yu, B. Hu, A. Dubrovkin, and Q. J. Wang, "Graphene-based tunable plasmonic Bragg reflector with a broad bandwidth," *Optics letters*, vol. 39, no. 2, pp. 271-274, 2014.
- [17] S. Asgari, A. Dolatabady, and N. Granpayeh, "Tunable midinfrared wavelength selective structures based on resonator with antisymmetric parallel graphene pair," *Optical Engineering*, vol. 56, no. 6, pp. 067102-067102, 2017.
- [18] M. Tamagnone, J. Gomez-Diaz, J. Mosig, and J. Perruisseau-Carrier, "Analysis and design of terahertz antennas based on plasmonic resonant graphene sheets," *Journal of Applied Physics*, vol. 112, no. 11, p. 114915, 2012.
- [19] M. A. Mansouri-Birjandi, M. Janfaza, and A. Tavousi, "Flat-Band Slow Light in a Photonic Crystal Slab Waveguide by Vertical Geometry Adjustment and Selective Infiltration of Optofluidics," *Journal of Electronic Materials*, journal article vol. 46, no. 11, pp. 6528-6535, 2017.
- [20] F. H. Koppens, D. E. Chang, and F. J. García de Abajo, "Graphene plasmonics: a platform for strong light–matter interactions," *Nano letters*, vol. 11, no. 8, pp. 3370-3377, 2011.
- [21] Q. Bao and K. P. Loh, "Graphene photonics, plasmonics, and broadband optoelectronic devices," *ACS nano*, vol. 6, no. 5, pp. 3677-3694, 2012.
- [22] J. Wang, X. Wang, C. Song, and X. Xia, "Ultracompact plasmonic sensor with graphene-based silicon reflector," in *Electro-Optical and Infrared Systems: Technology and Applications XIII*, 2016, vol. 9987, p. 99870X: International Society for Optics and Photonics.
- [23] W. Gao, J. Shu, C. Qiu, and Q. Xu, "Excitation of plasmonic waves in graphene by guided-mode resonances," *ACS nano*, vol. 6, no. 9, pp. 7806-7813, 2012.
- [24] X. Wang and J. Wang, "A Fabry-Perot plasmonic modulation with graphene-based silicon grating in mid-infrared region," in *SPIE/COS Photonics Asia*, 2016, pp. 1002813-1002813-7: International Society for Optics and Photonics.